



Contents lists available at SciVerse ScienceDirect

European Polymer Journal

journal homepage: www.elsevier.com/locate/europolj

Macromolecular Nanotechnology

High impact strength and low wear of epoxy modified by a combination of liquid carboxyl terminated poly(butadiene-co-acrylonitrile) rubber and organoclay

Wunpen Chonkaew^{a,b,*}, Narongrit Sombatsompop^c, Witold Brostow^{b,1}^a Department of Chemistry, Faculty of Science, King Mongkut's University of Technology Thonburi, 126 Pracha-utid Road, Bangmod, Thongkru, Bangkok 10140, Thailand^b Laboratory of Advanced Polymers & Optimized Materials (LAPOM), Department of Materials Science and Engineering and Center for Advanced Research & Technology (CART), University of North Texas, 3940 North Elm Street, Denton, TX 76207, USA^c Polymer Processing and Flow (P-PROF) Group, School of Energy, Environment and Materials, King Mongkut's University of Technology Thonburi, 126 Pracha-utid Road, Bangmod, Thongkru, Bangkok 10140, Thailand

ARTICLE INFO

Article history:

Received 6 August 2012

Received in revised form 4 March 2013

Accepted 15 March 2013

Available online 26 March 2013

Keywords:

Epoxy + clay hybrid composites

Epoxy modification

Dynamic friction

Wear

Dynamic mechanical analysis

Impact resistance

ABSTRACT

Hybrid composites with rubber properties were made from an epoxy modified with either 2.5 phr (parts per hundred) or 15 phr carboxyl terminated poly(butadiene-co-acrylonitrile) (CTBN). Organo-montmorillonite clay added ranged from 0 to 5 phr. Morphology including that of worn surfaces was examined, dynamic mechanical analysis performed and impact resistance determined. Dynamic friction and wear were determined using a pin-on-disc tribometer at dry sliding conditions. Storage modulus of the material containing 2.5 phr CTBN is higher than for 15 phr CTBN, a result of smaller CTBN droplets in the former. All composites have higher values of the Izod impact strength than the neat epoxy resin. Dynamic friction of the hybrids is not influenced by addition of clay whereas the wear resistance depends on the clay concentration. The wear rates at the applied load of 5 N for EP/15-CTBN hybrids are much larger than for EP/2.5-CTBN nanocomposites. This result can be related to the lower glassy storage modulus of EP/15-CTBN as compared to EP/2.5-CTBN. The addition of less than 5 phr clay improves the wear resistance at both 5 and 10 N normal loads. 1 phr clay in the EP/2.5-CTBN matrix is recommended as the optimum composition for improving both mechanical and tribological properties of the epoxy resin.

© 2013 Elsevier Ltd. All rights reserved.

1. Introduction

Epoxy resins have found uses in a variety of applications, such as adhesives, surface coatings, microelectronic capsulants and structural materials. Their widespread uses

are due in large part to their excellent adhesive, high chemical resistance, high temperature performances, as well as their ease of processing [1]. These resins are capable of high mechanical performance via increasing crosslink density of their networks. However, the highly crosslink density also inhibits molecular flow thus rendering the material low in toughness and poor in wear resistance. One of successful methods to enhance the toughness of rigid epoxy resins involves the modification of the uncured epoxy with the reactive rubbers [2–4]. Typically one applies a carboxyl-terminated butadiene acrylonitrile copolymer (CTBN rubber) to the uncured epoxy resin so as to obtain the rubber particles dispersed in the polymer matrix [5–8].

* Corresponding author at: Department of Chemistry, Faculty of Science, King Mongkut's University of Technology Thonburi, 126 Pracha-utid Road, Bangmod, Thongkru, Bangkok 10140, Thailand. Tel.: +66 24708843.

E-mail addresses: chonkaeww@gmail.com (W. Chonkaew), brostow@unt.edu (W. Brostow).

URLs: <http://www.unt.edu/LAPOM/> (W. Chonkaew), <http://www.unt.edu/LAPOM/> (W. Brostow).

¹ Tel.: +1 9405654358.

Rubber particles provide toughening, namely higher energy absorption by activating shear yielding, crack pinning, crack blunting or cavitation mechanisms [2,9–12]. A substantial amount of energy is dissipated within the plastic zone near the crack tip, resulting in improving toughness. By increasing the concentration of rubber phase, an increase in impact resistance of up to almost three times that of the unmodified epoxy has been reported [13–15]. Unfortunately, increased toughness could be achieved only up to a certain extent. Further addition of rubber particles results in worse mechanical properties [13,15]; among others, the flexural and Young modulae go down so that the epoxy resins become weak and are easily worn out [15]. In an earlier paper some of us reported a decrease of the storage modulus, impact strength and wear resistance as the CTBN rubber contents exceeded 5 parts per hundred (phr) [15]. Inorganic fillers including those with sizes in the nm range such as SiO₂, Al₂O₃, ZnO, silicate clay as well as glass fibers have been reported to improve modulae and wear resistance of epoxy resins [16–21]. On the other hand, inorganic fillers with high content can cause epoxy resins to become more brittle. When inorganic hard phases are added to increase stiffness, there is a corresponding decrease in strain at break ϵ_b [22,23]. We recall that ϵ_b is inversely proportional to brittleness B [24,25].

Among the different kinds of nanofillers, montmorillonite-based clay is one of those commonly applied to epoxy resins. The fabrication of polymer clay composites, like other inorganic fillers, can easily result in agglomeration of clay causing worsening of mechanical properties and wear resistance. However, the polymer + clay composites with exfoliated clay platelets have been reported to provide higher modulus than those consisting of conventional micron-scale fillers of the same chemical composition [26,27]. The improved dispersion of clay in the epoxy matrix by modifying clay surface caused a decrease in friction and specific wear rate [28].

To combine the benefits of each additive, combinations of rubber and clay have been used. Balakrishnan et al. [29] added modified organic montmorillonite clay to a dispersion of preformed acrylic rubber particles in an epoxy. They found that when both additives were present in epoxy resin, ductility was enhanced without compromising modulus and strength. The amounts of clay and dispersion of clay aggregates in the epoxy matrix were found to be sensitive to clay and rubber concentrations, and clay preferentially adsorbed to the rubber particles. Marouf et al. [30] added core-shell rubber particles and organically modified clay to an epoxy resin. They found that the compressive yield strength was independent of organoclay content up to 5 phr but there was a significant decrease in fracture toughness. Moghbelli et al. [31] studied the effects of nanoscale core-shell rubber particles and α -zirconium phosphatase nanoplatelet fillers on the scratch behavior of epoxy. They found that the introduction of either nanoparticles or nanoplatelets alone had little effect and a combination of both types of fillers was needed to improve scratch resistance.

Overall, much more work has been and is being done on mechanical properties of polymer-based composites than on their tribological properties. This while low friction,

high scratch and wear resistance have not only technical but also large economic significance for industry [32–35]. In this situation, and in particular taking into account some earlier results [15], we have now created epoxy based nanohybrids containing 2.5 and 15 phr (carboxyl terminated poly(butadiene-co-acrylonitrile) (CTBN) and clay. Our objective was improvement of tribological and mechanical properties of epoxies at the same time.

2. Experimental

2.1. Materials

We have used diglycidyl ether of bisphenol A (DGEBA) namely EPON 828 with epoxy equivalent weight of 185–192 g/eq. The hardener used was a cycloaliphatic amine (EPIKURE 3383) with the equivalent weight of 114 g/eq. Both chemicals were from Hexion™ Speciality Chemicals, USA. The reactive liquid rubber was carboxyl-terminated acrylonitrile butadiene copolymer (CTBN) with number average molecular weight $M_n = 3.8 \times 10^3$ containing acrylonitrile of 8–12 wt.% from Aldrich, Singapore. The clay used was surface modified montmorillonite containing 0.5–5 wt.% aminopropyl triethoxysilane and 15–35 wt.% octadecylamine (Nanomer® I31PS) from Aldrich, Singapore. All chemicals were used as received without further purification.

2.2. Preparation of epoxy based hybrid composites

DGEBA epoxy was mixed with 2.5-phr or 15-phr of liquid CTBN rubber at 80 °C for 30 min with mechanical stirring at 8000 rpm. Organically modified montmorillonite clay was heated in a conventional oven at 80 °C to eliminate moisture. Then known amounts of clay (0.5, 1, 3 or 5 phr) were gradually added to each epoxy + CTBN mixture, and stirred mechanically for 30 min at room temperature. The mixtures of epoxy, CTBN and clay were then degassed in a vacuum oven and ultrasonicated to remove the entrapped bubbles. After the sonication, the stoichiometric quantity of curing agent was then added prior to hand mixing for 3–5 min. Finally the mixtures were poured into molds and cured at 25 °C for 16 h and post cured at 100 °C for 2 h as recommended by a manufacturer of the neat epoxy resin.

2.3. Materials characterization and mechanical testing

2.3.1. X-ray diffractometry

X-ray diffraction analysis (XRD) was carried out on the clay powder and on the epoxy composites. The measurements were performed at room temperature on a Bruker D 8 Discover X-ray diffractometer (Germany), using Cu K α radiation. The samples were scanned in 2θ range of 1–30° in steps of 0.02° and with 0.4 s/step. The interlayer spacing of clay containing in the hybrids was calculated using the Braggs equation.

2.3.2. Impact testing

Izod impact tests were performed at room temperature using a pendulum impact tester (Yasuda Seiki Seisakusho

9347, Intro Enterprise) according to ASTM D256-10. At least five specimens were tested and the average results are reported below.

2.3.3. Morphology characterization

Transmission electron microscopy (TEM) samples were cut from undeformed specimens using an ultramicrotome equipped with a diamond knife. The microtomed samples were collected in a trough filled with water and lifted out of water using copper grids. The structure of dispersed clay and rubber in nanocomposites was investigated using a TEM (FEI Technai F20 TEM, USA) operating at a voltage of 120 kV.

The fracture surfaces obtained from the impact tests were investigated using a scanning electron microscope (SEM) (JEOL JSM-6610, Japan) with 15 kV working energy. All the surfaces were gold coated to prevent the charging before the surface observation and examined at a magnification of 1500 \times .

2.3.4. Dynamic mechanical analysis

Storage modulus E' and $\tan\delta$ were determined using a dynamic mechanical analyzer (Mettler Toledo, DMA/SDTA 861e, Switzerland). Specimens of rectangular shape ($63 \times 12 \times 3 \text{ mm}^3$) were analyzed in 3-point-bending mode. The measurements were carried out from -20°C to $+130^\circ\text{C}$ with $3^\circ\text{C}/\text{min}$ of heating rate, at the 1.0 Hz frequency.

2.3.5. Tribological testing

We have used a pin-on-disc tribometer (CSM Instruments, Peseux, Switzerland, model 18-272) at ambient conditions. The wear track radius R and the ball end spherical radius r were 6.0 mm and 3.18 mm, respectively. The sample surface was rubbed against a stainless steel ball (SKF, Thailand), with sliding velocities of 0.10 m/s for 500 m under the applied loads of 5.0 N ($p = 0.172 \text{ GPa}$) and 10.0 N ($p = 0.217 \text{ GPa}$). The dynamic friction μ was obtained using Amonton's first law of friction, namely:

$$\mu = F/W, \quad (1)$$

where F is the tangential force and W is the normal force in the unit of N.

To determine the wear damage, worn surfaces were analyzed using an optical microscope. The wear volume loss V in mm^3 was calculated from the wear track width d in mm as:

$$V = 2\pi R[r^2 \sin^{-1}(d/2r) - (d/4)(4r^2 - d^2)^{1/2}] \quad (2)$$

The wear rate Z in $\text{mm}^3/\text{N m}$ was calculated as:

$$Z = V/(Ws), \quad (3)$$

where s is sliding distance in m.

The wear mechanisms were investigated on worn surfaces using scanning electron microscope model of JEOL JSM-6610, Japan, with 10 kV working energy at magnification of 250 \times . Again gold coating was applied to prevent the charging before the surface observation.

3. Diffractometry results

Fig. 1a shows the XRD pattern for clay, epoxy resin, the rubber modified epoxy resins having CTBN of 2.5 phr and 15 phr (EP/2.5-CTBN and EP/15-CTBN), and the hybrid composites containing 0.5-phr clay (EP/2.5-CTBN + 0.5-clay and EP/15-CTBN + 0.5-clay). The XRD pattern of the clay shows a strong peak at about $2\theta = 4.00^\circ$ corresponding to an interlayer spacing (d_{001}) of 22.07 Å. A weak peak at $2\theta = 8.00^\circ$, corresponding to a (002) reflection and at $2\theta = 19.78^\circ$, corresponding to (100) reflection have been found. A broad peak between 2θ to 23° revealing the presence of the amorphous silane has been observed. The XRD patterns of the rubber modified epoxy containing CTBN of 2.5 and 15 phr show two broad reflection peaks of amorphous CTBN rubber and epoxy resin. When 0.5 phr clay was added, the reflection peak due to the interlayer spacing (d_{001}) of clay disappeared. A similar observation in the case of epoxy/layered silicate composites was reported by others [36,37]. The absence of the characteristic clay (d_{001}) peak indicates the exfoliation of the clay platelets in the CTBN modified epoxy matrix. However, when 1 phr clay is added, the XRD patterns of the EP/CTBN + clay composites become combinations of the XRD pattern of clay and the rubber modified epoxy; see Fig. 1b. The peak due to the interlayer spacing (d_{001}) of clay is weak and shifted to $2\theta = 3.17^\circ$ ($d_{001} = 27.87 \text{ Å}$) for the hybrid composite of EP/2.5-CTBN + 1-clay and to $2\theta = 3.09^\circ$ ($d_{001} = 28.58 \text{ Å}$) for EP/15-CTBN + 1-clay. The results indicate a significant increase in the interlayer spacing, but not complete delamination. The presence of the characteristic clay (001) peak at a lower 2θ indicates that a portion of clay has been intercalated. The interlayer spacing (d_{001}) of clay in the hybrid composites increases with further adding clay, but then decrease upon the addition of 5 phr; the respective values are still lower than that of clay powder.

4. DMA results

DMA parameters as a function of temperature are shown in Fig. 2. All the composites of EP/15-CTBN and clay have lower storage modulae than the composites of EP/2.5-CTBN and clay. This might be related to the fact that the modulus of the EP/15-CTBN is much lower than that of the EP/2.5-CTBN resin, apparently a result of larger CTBN droplets to be discussed in Section 6. The storage modulae and a glass transition temperatures T_g obtained from the $\tan\delta$ maxima for the neat epoxy resin, EP/2.5-CTBN and EP/15-CTBN are listed in Table 1.

Fig. 2a shows the storage moduli of the hybrid composites of EP/2.5-CTBN containing 0, 0.5, 1.0, 3.0 and 5.0 phr clay as a function of temperature. Apparently clay containing hybrids have lower storage modulae in the glassy state for 0.5 and 1.0 phr. The result is unexpected; clay can lower stiffness and load bearing capability of the CTBN modified epoxy resin. This result can be explained by a reaction between epoxy DGEBA and the $-\text{NH}_2$ amino groups on the surfaces of clay particles – instead of between DGEBA and the cycloaliphatic amine hardener; the

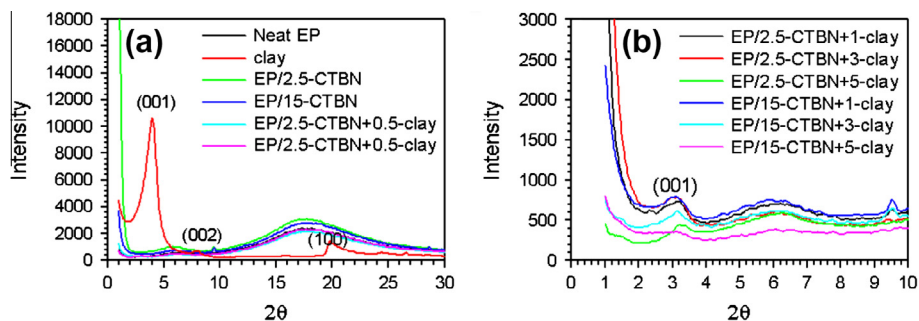


Fig. 1. XRD of the powder clay, EP/2.5-CTBN, EP/15-CTBN and the hybrid composites.

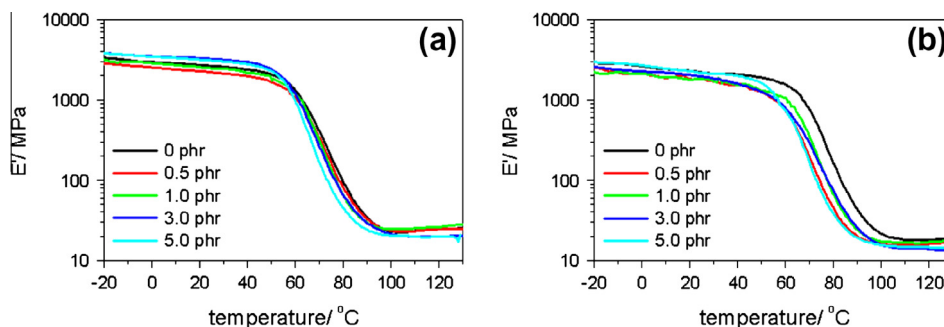


Fig. 2. Temperature dependence of storage modulus E' of the epoxy based hybrids with EP/2.5-CTBN (a) and EP/15-CTBN (b) containing 0.5, 1, 3 and 5 phr clay.

Table 1

Properties of neat epoxy resin and the epoxy modified with CTBN.

Sample	Storage modulus at 25 °C (GPa)	T_g (°C)
Epoxy resin	3.9	83.5
EP/2.5-CTBN	2.7	77.8
EP/15-CTBN	2.2	80.9

result is a reduction in crosslink density. However, there is a reinforcement effect when 3 or 5 phr clay, a stiff material, is added. The glassy storage moduli at 25 °C increase about 23% and 18% when adding 3 or 5 phr clay, respectively. The addition of higher stiffness clay should be one of the possible explanations for the increase in glassy storage modulus at higher clay content. The values of glassy state storage moduli of the composites with 3 and 5 phr clay are still lower than that of the neat epoxy (3.9 GPa).

Fig. 2b shows the storage moduli of the hybrid composites of EP/15-CTBN containing 0, 0.5, 1.0, 3.0 and 5.0 phr clay as a function of temperature. Like the EP/2.5-CTBN + clay hybrids, a reduction in glassy storage modulus is also found in case of EP/15-CTBN + clay composites, while a reinforcement is found at high clay content. The addition of 3 phr clay lowers glassy storage modulus of the EP/15-CTBN resin, whereas the reinforcement is observed due to the addition of 5 phr clay.

Figs 3a and b shows $\tan \delta$ diagrams in the temperature range from -20 to $+130$ °C. A single peak is observed for all epoxy composites systems. Glass transition temperatures T_g identified from the peaks in $\tan \delta$ shift to lower temperatures as compared with the CTBN modified epoxy

resins. T_g values for the hybrids made with EP/2.5-CTBN decrease with increasing amounts of clay. There are several explanations for the T_g reduction [38,39]. One is a plasticizing effect of the epoxy network by surface modifiers in the organoclay [39]. A homopolymerization of sorts of DGEBA epoxy has been hypothesized – due to the catalytic effect of alkylammonium ions during the mixing stage and hence changes in the cured networks [38,39]. Also the presence of clay might cause stoichiometric imbalances leading to formation of imperfect networks [39]. Moreover, in case of our hybrid composites, lower crosslink density reflected in the T_g reduction may be a result of a reaction of the surface modifiers and DGEBA epoxy, leading to stoichiometric imbalances. One can further speculate that formation of regions with lower crosslink density is related to silicate galleries or regions close to the CTBN or silicate layers – reflected by the reduction in T_g as the clay contents increases. For EP/15-CTBN + clay composites, changes in T_g do not depend on the clay content. However, all the hybrid composites made with EP/15-CTBN have at least 5 °C lower T_g values than the EP/15-CTBN without clay. Agglomeration of clay at high loadings, leading to improved chain mobility together with an imperfect epoxy network is one more explanation.

5. Impact strength results

The relationship between the clay content and notched Izod impact strength per unit width of the specimen is shown in Fig. 4. The addition of 0.5 phr clay significantly improves the impact strength of EP/2.5-CTBN and EP/15-

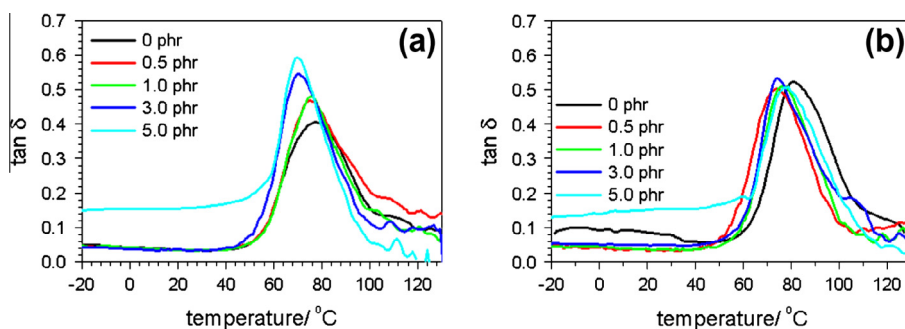


Fig. 3. Temperature dependence of $\tan \delta$ of the hybrids with EP/2.5-CTBN (a) and EP/15-CTBN (b) containing 0.5, 1, 3 and 5 phr clay.

CTBN materials, but then the values gradually decrease with further addition of clay. However, all composites have higher values of impact strength than the neat epoxy resin. One of the possible reasons for the increased impact strength is the increased ability of the matrix to yield, as evident by the reduction in T_g seen in DMA. The yielding of the matrix is related to a decrease of the local stress concentrations. Consequently, higher applied loads are required to produce fracture. An increased amount of the clay hard phase causes a gradual reduction of impact resistance at the high clay contents. See below an explanation based on SEM fractographs provided in Figs. 6 and 7.

6. SEM and TEM results for fracture surfaces

Pertinent SEM fractographs are shown in Fig. 5.

Fig. 5a shows the fracture surface of the neat epoxy. A smooth glassy surface with occasional river patterns is observed. This result indicates brittle fracture at room temperature of the neat epoxy, which accounts for its poor impact strength. The fractographs of the epoxy resins modified with 2.5 phr CTBN and 15 phr CTBN (EP/2.5-CTBN and EP/15-CTBN) shown in Fig. 5b and c demonstrate a two-phase morphology in which the precipitated CTBN rubber particles are dispersed throughout the epoxy matrices. Cavitation and debonding are observed and provide toughening mechanisms. Cavitation here is the formation of holes because of the presence of the rubber. As discussed in a previous study [15], the size of the CTBN rubber in-

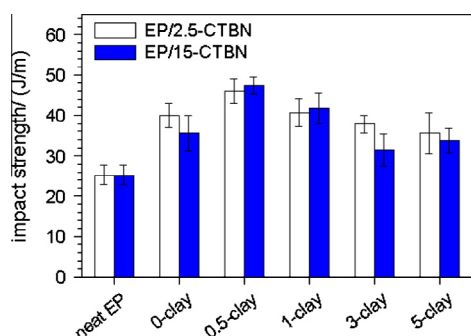


Fig. 4. Impact strength values of the neat epoxy and hybrids composites made with either EP/2.5-CTBN or EP/15-CTBN containing 0, 0.5, 1, 3 and 5 phr clay.

creases with increasing rubber content. This is seen here as well, the size of rubber phase is larger in the EP/15-CTBN sample than in the EP/2.5-CTBN sample. The increases in size of dispersed phase are associated with the agglomeration or coalescence of the rubber particles at high rubber content, leading to lower impact strength and lower storage modulus of the EP/15-CTBN. In other words, the internal cohesion of the matrix is affected less by smaller CTBN particles; larger rubber particles provide disruption of the matrix.

Figs. 6 and 7 show the SEM fractographs of the hybrids containing different amounts of clay. We find that the toughening mechanisms of the hybrids both with EP/2.5-CTBN and with EP/15-CTBN vary with the clay concentration. On adding 0.5 phr clay (Figs. 6a and 7b), the crack pinning is observed together with cavitations and rubber debonding. Moreover, there are traces of clay aggregates around the boundaries of the spherical holes that are formed by pulling out CTBN rubber particles. These results confirm that adsorption of clay on the surface of the rubber particles takes place. The clay particles aligned along the interface of CTBN rubber and epoxy result in the formation of core (rubber)–shell (clay) structure. The morphology observed at this low amount of organoclay and rubber agrees with the already mentioned results of Balakrishnan et al. [29]. Putting in 1 phr clay (Figs. 6b and 7b) limits the rubber pull out – while the cavitations have smaller sizes. Clay at the interface provides bridges between CTBN and epoxy phases, resulting in better adhesion between these phases. When we put in 3 phr or 5 phr clay, cavitations and material pull-out are not observed. Some fractions of clay diffuse and agglomerate inside the CTBN droplets. The CTBN particles then become more brittle, the materials fracture more easily under impact – as we have seen in Fig. 4. At these clay concentrations cracks are not suppressed by the rubber particles but go through the rubber particles. We have a process that might be called flexibilization of the matrix – resulting in lower storage modulus and lower impact strength values.

More evidence concerning the morphology of our composites was obtained from a TEM study on the ultra-microtomed specimens (Fig. 8). The presence of core–shell structure is seen as dark round phases in the micrograph when a small amount of clay was added to the epoxy mixed with preformed rubbers at both low and high rubber contents; see Fig. 8a and b. We have found that

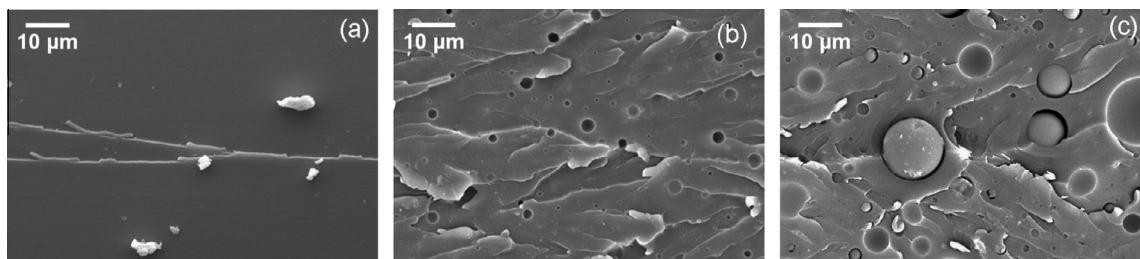


Fig. 5. SEM fractographs of the neat epoxy resin (a), the epoxy modified with CTBN 2.5 phr (b) and 15 phr (c).

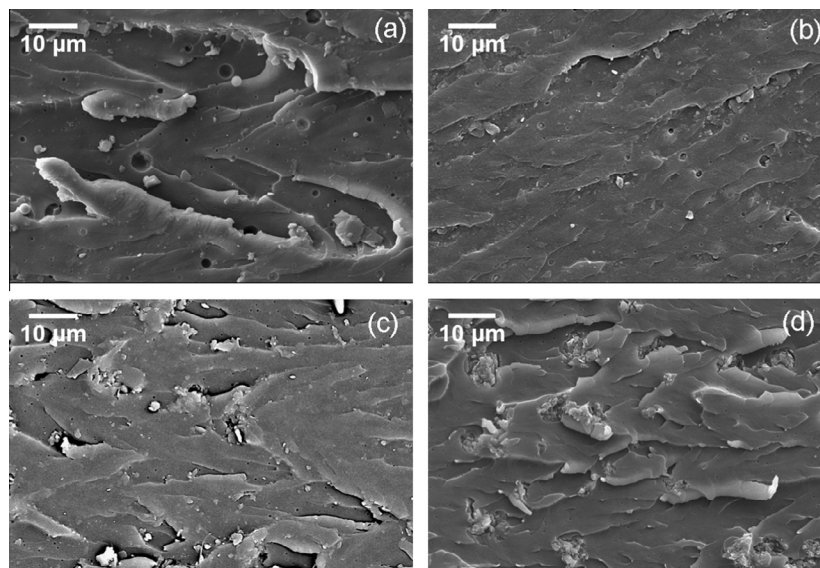


Fig. 6. SEM fractographs of the epoxy hybrids with 2.5-phr CTBN containing 0.5 phr clay (a), 1 phr clay (b), 3 phr clay (c) and 5 phr clay (d).

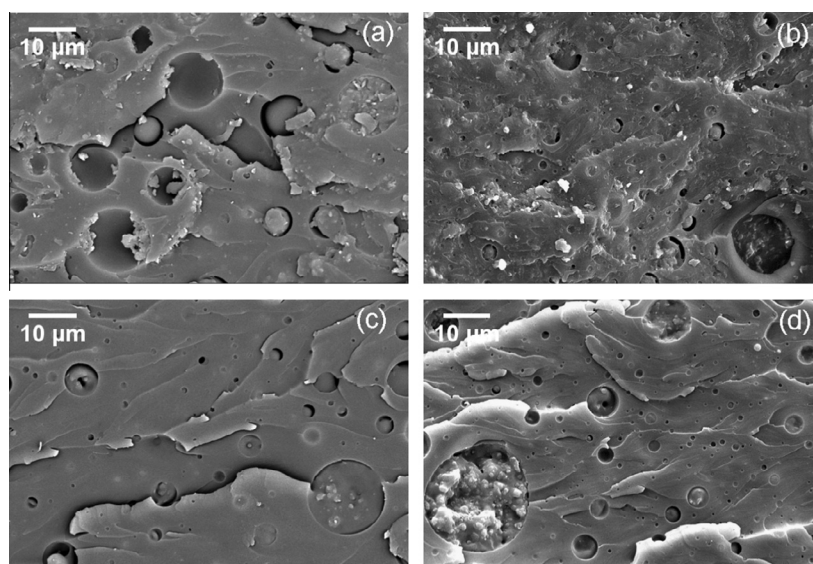


Fig. 7. SEM fractographs of the epoxy hybrids with 15-phr CTBN containing 0.5 phr clay (a), 1 phr clay (b), 3 phr clay (c) and 5 phr clay (d).

the clay platelets align along the interfaces of the rubber particles. When larger amounts of clay are added, the clay particles diffuse into the rubber particles and agglomerate in the epoxy matrix; see Fig. 8c.

7. Dynamic friction and wear

Dynamic friction measurements have been performed as described in Section 2, results are presented in Figs. 9 and 10. As usual in pin-on-disk tribometry, there is an initial period before a certain level of friction is seen.

We see that dynamic friction values for our hybrids under a load of 10 N are lower than those under 5 N. Changes in friction as a function of clay concentration are not significant, although one notices a slight increase with increasing clay concentration for 5 N and even less change for 10 N.

Interesting is a certain decrease in friction with sliding distance for the hybrids with EP/15-CTBN containing higher concentrations of clay under the load of 10 N (Fig. 10b). One possible explanation is a softening/melting mechanism due to frictional heat. Polymers are known to have low thermal conductivity; a result is high sliding interfacial temperature. Thermal softening and the associated increase in the real contact area cause the friction to rise above T_g . However, as discussed by Steijn [40], there is lubrication by a molten polymer film if the sliding interfacial temperature locally exceeds the melting point T_m .

Wear tracks obtained in pin-on-disk testing were investigated; wear was calculated from Eq. (2) and wear rates from Eq. (3). The results are shown in Fig. 11.

The wear rates at the applied load of 5 N of EP/15-CTBN hybrids are much larger than for EP/2.5-CTBN. This result seems related to the low glassy storage moduli of EP/15-CTBN as compared to those of EP/2.5-CTBN; see again Table 1. We see in Fig. 11a that the EP/2.5-CTBN hybrid with 1 phr clay has very high wear resistance, that is the lowest wear rate. A further increase in clay concentration increases the wear rate; for 5 phr clay the value is even higher than for the neat epoxy resin. This can be explained by agglomeration of the clay inside the CTBN particles, resulting in a composite more vulnerable to the applied load as previously discussed; see again Figs. 6d and 7d.

Then material removal takes place by the cutting action of the asperities of the ball counterface [41]. The debris containing clay also acts as an abrasive, resulting in more material removal and increased wear rate [42].

At the applied load of 10 N, wear rate values are much larger than at 5 N. This of course is expected. The lowest wear rate belongs to the EP/15-CTBN hybrid with 1 phr clay. The wear rates of EP/2.5-CTBN and EP/15-CTBN decrease significantly with the addition of clay, but then increase to a higher value than for the neat epoxy resin at 5 phr clay. We recall the core-shell morphology at low clay content discussed in Sections 5 and 6. The improved wear resistance of the EP/15-CTBN as compared to the neat epoxy is attributed to these phenomena.

In Section 6 we have considered SEM results for fracture surfaces. We have now studied by SEM worn surfaces after pin-on-disk testing at 5.0 N load. The results are presented in Fig. 12.

The 2.5-CTBN modified resin (Fig. 12a) exhibits the scale-like damage pattern, apparently generated under a repeating load during sliding [16,21,41]. For 1 phr clay (Fig. 12b) the transfer film left traces on the surface of the track, an evidence for an adhesive type of wear mechanism. For 3 phr clay (Fig. 12c), cracks across the wear tracks occur together with material waves. For 5 phr clay (Fig. 12d), the damage produced on the worn surface is discontinuous. Inhomogeneous material waves as well as cracks are seen inside the track. Apparently uneven stress concentrations built up inside this composite, possibly a consequence of the inhomogeneity of the stress.

We show in Fig. 13 results for materials containing the EP/15-CTBN resin. We see scale-like damage together with the delamination on the wear track of EP/15-CTBN (Fig. 13a). The damages of the surface are more severe than those observed for the EP/2.5-CTBN materials. The addition of 1 phr clay mitigated the surface damages – as can be seen from the reduction of the width of wear track. The ploughing grooves were found besides the scale pattern when clay was added. A possible mechanism of formation of these grooves involves ploughing the epoxy surface by the work-hardened transfer particles [42]. As the clay content increased to 3 phr (Fig. 13c), the cracks are arrested by the clay platelets, so that the crack formation and material waves are rarely observed. For 5 phr clay, the ploughing

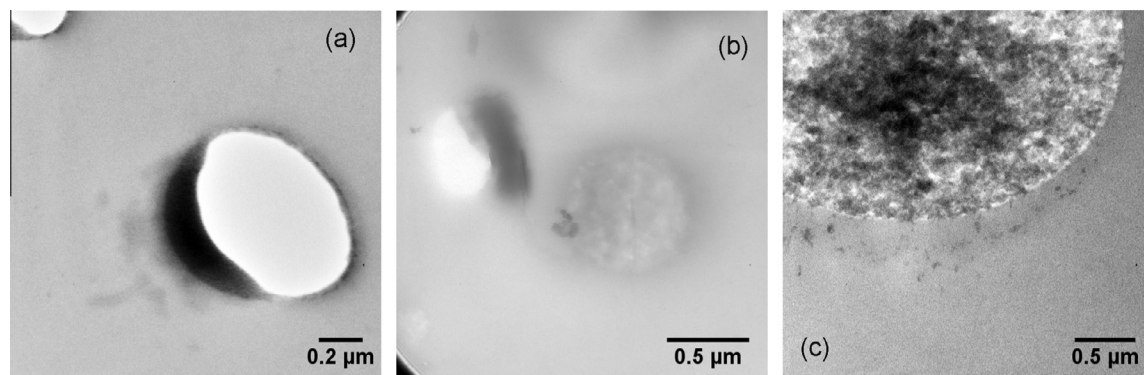


Fig. 8. TEM micrographs of: (a) EP/2.5-CTBN + 0.5 clay; (b) EP/15-CTBN + 0.5 clay; and (c) EP/15-CTBN + 1 clay.

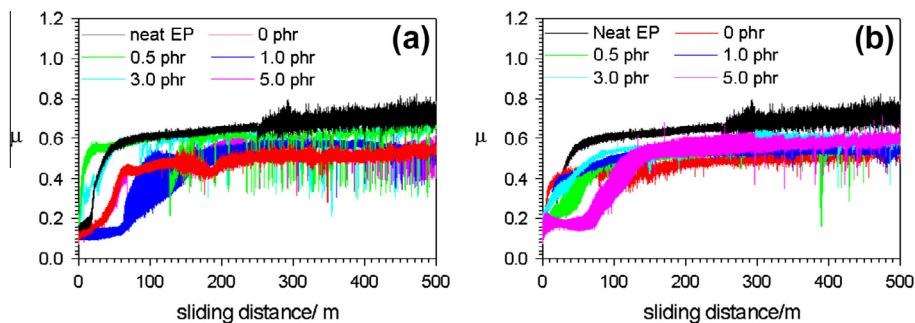


Fig. 9. Dynamic friction of the neat epoxy resin and hybrids with EP/2.5-CTBN (a) and again the neat resin and hybrids with EP/15-CTBN (b) at the load of 5.0 N. The hybrids contain 0 phr, 0.5 phr, 1 phr, 3 phr and 5 phr clay.

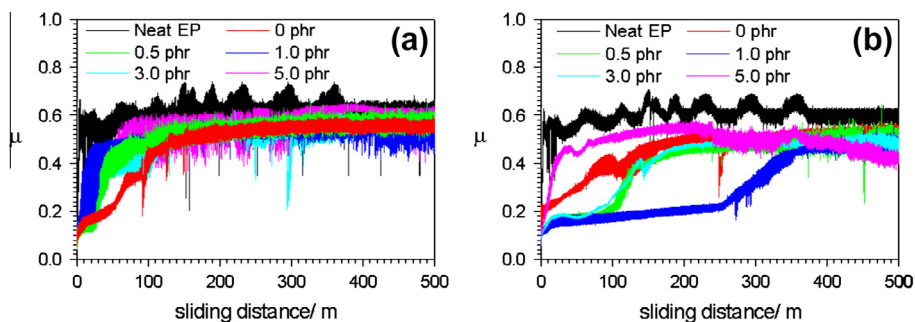


Fig. 10. Results analogous to those in Fig. 9 but now for the load of 10.0 N.

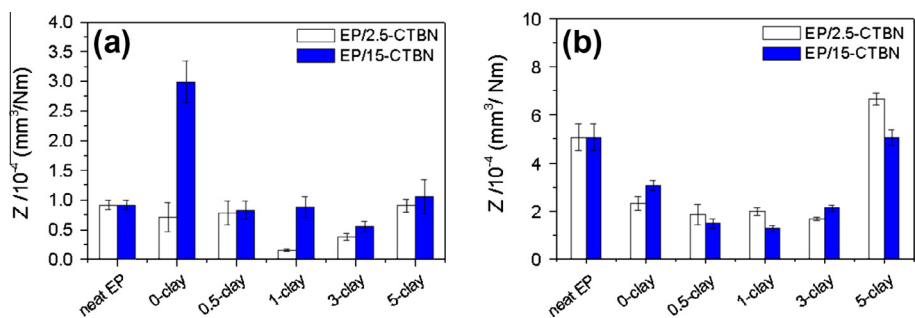


Fig. 11. Wear rates at the applied load of 5.0 N (a) and 10.0 N (b).

grooves are more evident. This can be explained by poor interaction of fillers and epoxy matrix due to the agglomeration of clay. Under the applied load of 10 N, the scale-like damage pattern and the surface peeling off due to the fatigue wear mechanism are found on the tracks of the EP/2.5-CTBN resin and EP/2.5-CTBN + 0.5-clay hybrids. Wear mechanisms similar to those under 5 N but more severe are observed (the respective figure is not included here).

8. A survey of results

We have determined properties for epoxies containing organoclay at several concentrations and either 2.5 phr or 15 phr CTBN rubber. The rubber phase lowers the storage modulus while it enhances the impact strength. Impact strength increases upon adding 0.5 or 1.0 phr clay but de-

creases upon further addition of clay. Low concentrations of clay can be used to develop epoxy composites with good impact strength and satisfactory stiffness at the same time.

Dynamic friction of our hybrids is only weakly influenced by the addition of clay, while the wear resistance depends on the addition and significantly lower wear rates are seen. As already noted, the formation of core-shell morphology is a reason for the improved wear resistance of the hybrids at the low clay content; this effect is more significant at the higher rubber content, that is for EP/15-CTBN. Wear mechanisms include adhesion, abrasion and fatigue-delamination, together with thermal softening. To optimize properties, we recommended that 1 phr clay in the preformed EP/2.5-CTBN matrix should be used for improving both mechanical and tribological properties of epoxy resins.

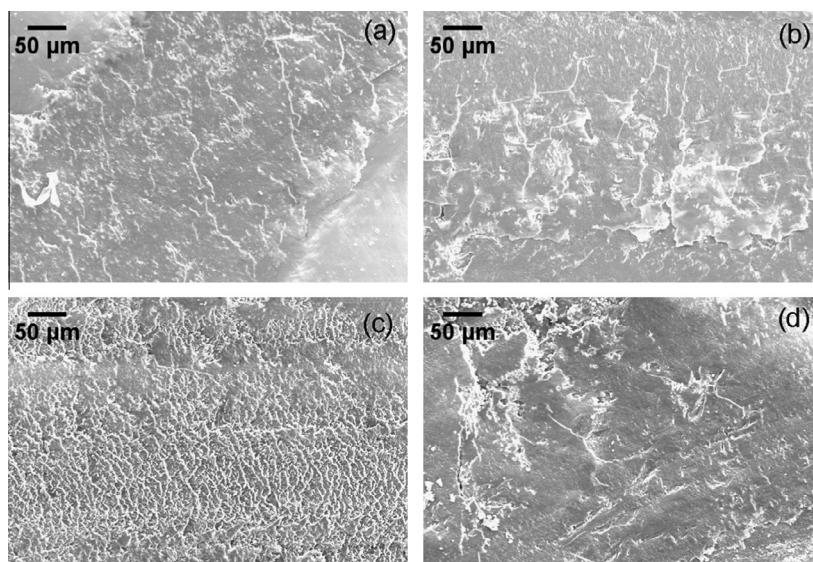


Fig. 12. SEM micrographs of worn surfaces: EP/2.5-CTBN resin (a), EP/2.5-CTBN and clay containing 1 phr clay (b), 3 phr clay (c) and 5 phr clay (d) after sliding against a stainless steel ball with the applied load of 5.0 N.

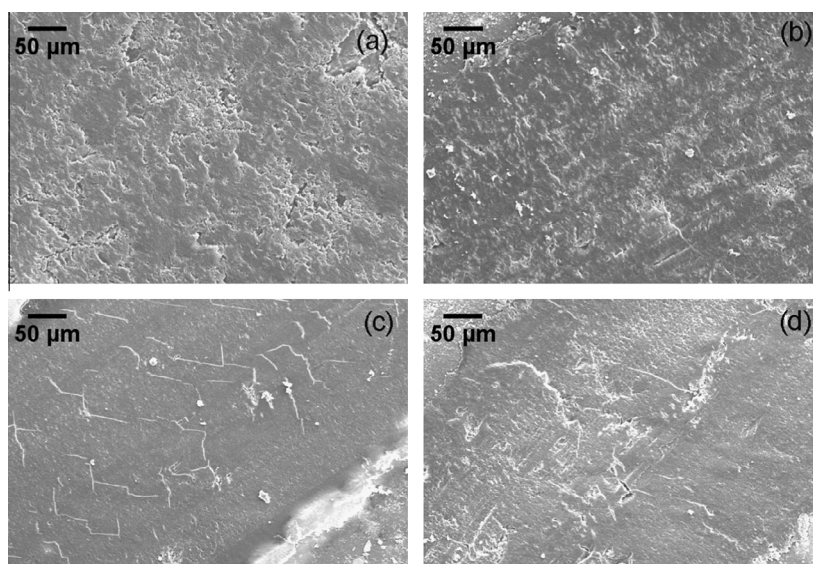


Fig. 13. SEM micrographs of worn surfaces: the EP/15-CTBN resin (a), hybrids of EP/15-CTBN and clay containing 1 phr clay (b), 3 phr clay (c) and 5 phr clay (d) after sliding against a steel ball with the applied load of 5.0 N.

Epoxy resins have a large variety of applications [1,43], hence our hybrids can be used for a variety of purposes. From a broader point of view, our results illustrate statements made by Kopczynska and Ehrenstein [44], Desai and Kapral [45] and also by Michler and Balta Calleja [46] on the importance of interfaces for properties of multiphase materials containing polymers.

Acknowledgements

This work was financially supported by the Thailand Research Fund (MRG-5380129). The authors are grateful to the East Asiatic (Thailand) Public Co., Ltd. for supplying

epoxy and its hardener and to the National Research University (NRU) and the Office of Higher Education Commission (OHEC) of Thailand, Bangkok. Authors also gratefully acknowledge the Center for Advanced Research and Technology (CART) at the University of North Texas (UNT) and the help of Dr. Soumya Nag and Dr. David Garrett in the TEM study.

References

- [1] Bilyeu B, Brostow W, Menard KP. Epoxy thermosets and their applications. I. Chemical structures. *J Mater Educ* 1999;21:281; Bilyeu B, Brostow W, Menard KP. Epoxy thermosets and their applications. II. Thermal analysis. *J Mater Educ* 2000;22:107;

- Bilyeu B, Brostow W, Menard KP. Epoxy thermosets and their applications. III. Kinetic equations and models. *J Mater Educ* 2001;23:189.
- Bratychak M, Shyshchak O, Bratychak MM. Synthesis of peroxy oligomers on the basis of epoxy compounds in presence of tert-butylperoxymethanol. *Chem & Chem Tech* 2007;1:15.
- [2] Ozturk A, Kaynak C, Tincer T. Effects of liquid rubber modification on the behaviour of epoxy resin. *Eur Polym J* 2001;37(12):2353–63.
- [3] Chikhi N, Fellahi S, Bakar M. Modification of epoxy resin using reactive liquid (ATBN) rubber. *Eur Polym J* 2002;38:251–64.
- [4] Ratna D, Simon GP. Mechanical characterization and morphology of carboxyl randomized poly(2-ethyl hexyl acrylate) liquid rubber toughened epoxy resins. *Polymer* 2001;42:7739–47.
- [5] Kunz SC, Sayre JA, Assink RA. Morphology and toughness characterization of epoxy resins modified with amine and carboxyl terminated rubbers. *Polymer* 1982;23(13):1897–906.
- [6] Kinloch AJ, Shaw SJ, Tod DA, Hunston DL. Deformation and fracture behaviour of a rubber-toughened epoxy: 1. Microstructure and fracture studies. *Polymer* 1983;24:1341–53.
- [7] Bartlet P, Pascault JP, Sautereau H. Relationships between structure and mechanical properties of rubber-modified epoxy networks cure with dicyanodiamide hardener. *J Appl Polym Sci* 1985;30:2955–66.
- [8] Pearson RA, Yee AF. Toughening mechanisms in elastomer-modified epoxies. Part 2: Microscopy studies. *J Mater Sci* 1986;21:2475–88.
- [9] Verchere D, Sautereau H, Pascault JP, Moschiar SM, Riccardi CC, Williams RJJ. Miscibility of epoxy monomers with carboxyl-terminated butadiene-acrylonitrile random copolymers. *Polymer* 1989;30(1):107–15.
- [10] Chen TK, Jan YH. Toughening mechanism for a rubber-toughened epoxy resin with rubber/matrix interfacial modification. *J Mater Sci* 1991;26:5848–58.
- [11] Wise CW, Cook WD, Goodwin AA. CTBN rubber phase precipitation in model epoxy resins. *Polymer* 2000;41:4625–33.
- [12] Pearson RA, Yee AF. Influence of particle size and particle size distribution on toughening mechanisms in rubber-modified epoxies. *J Mater Sci* 1991;26(14):3828–44.
- [13] Tripathi G, Srivastava D. Effect of carboxyl-terminated poly(butadiene-co-acrylonitrile) (CTBN) concentration on thermal and mechanical properties of binary blends of diglycidyl ether of bisphenol-A (DGEBA) epoxy resin. *Mater Sci Eng A* 2007;443:262–9.
- [14] Yu S, Hu H, Ma J, Yin J. Tribological properties of epoxy/rubber nanocomposites. *Tribol Int* 2008;41(12):1205–11.
- [15] Chonkaew W, Sombatsomporn N. Mechanical and tribological behaviors of epoxy modified by carboxyl-terminated poly (butadiene-co-acrylonitrile) rubber. *J Appl Polym Sci* 2012:361–9.
- [16] Durand JM, Vardavoulias M, Jeandin M. Role of reinforcing ceramic particles in the wear behaviour of polymer-based model composites. *Wear* 1995;181–183:833–89.
- [17] Zhang MQ, Rong MZ, Yu SL, Wetzel B, Friedrich K. Effect of particle surface treatment on the tribological performance of epoxy based nanocomposites. *Wear* 2002;253:1086–93.
- [18] Wetzel B, Hauptert F, Zhang MQ. Epoxy nanocomposites with high mechanical and tribological performance. *Compos Sci Technol* 2003;63(14):2055–67.
- [19] Wang K, Chen L, Kotaki M, He C. Preparation, microstructure and thermal mechanical properties of epoxy/crude clay nanocomposites. *Composites Part A* 2007;38:192–7.
- [20] Larsen T, Andersen TL, Thorning B, Vigild ME. The effect of particle addition and fibrous reinforcement on epoxy-matrix composites for severe sliding conditions. *Wear* 2008;264(9–10):857–68.
- [21] Brostow W, Chonkaew W, Datashvili T, Menard KP. Tribological properties of epoxy + silica hybrid materials. *J Nanosci Nanotechnol* 2009;9:1916–22.
- [22] Prasad SV, Calvert PD. Abrasive wear of particle-filled polymers. *J Mater Sci* 1980;15:1746–54.
- [23] Cirino M, Pips RB, Friedrich K. The abrasive wear behaviour of continuous fibre polymer composites. *J Mater Sci* 1987;22(7):2481–92.
- [24] Brostow W, Hagg Lobland HE, Narkis M. Sliding wear, viscoelasticity and brittleness of polymers. *J Mater Res* 2006;21:2422–8.
- [25] Brostow W, Hagg Lobland HE, Narkis M. The concept of materials brittleness and its applications. *Polym Bull* 2011;59:1697–707.
- [26] Giannelis EP. Polymer-layered silicate nanocomposites: synthesis, properties and applications. *Appl Org Chem* 1998;12:675–80.
- [27] Ha SR, Ryu SH, Park SJ, Rhee KY. Effect of clay surface modification and concentration on the tensile performance of clay/epoxy nanocomposites. *Mater Sci Eng A* 2007;448:264–8.
- [28] Ha SR, Rhee KY. Effect of surface-modification of clay using 3-aminopropyltriethoxysilane on the wear behavior of clay/epoxy nanocomposites. *Colloids Surf A* 2008;322:1–5.
- [29] Balakrishnan S, Start PR, Raghavan D, Hudson SD. The influence of clay and elastomer concentration on the morphology and fracture energy of preformed acrylic rubber dispersed clay filled epoxy nanocomposites. *Polymer* 2005;46(25):11255–62.
- [30] Marouf BT, Pearson RA, Bagheri R. Anomalous fracture behavior in an epoxy-based hybrid composite. *Mater Sci Eng A* 2009;515(1–2):49–58.
- [31] Moghbelli E, Sun L, Jiang H, Boo WJ, Sue H-J. Scratch behavior of epoxy nanocomposites containing α -zirconium phosphate and core-shell rubber particles. *Polym Eng Sci* 2009:483–90.
- [32] Myshkin NK, Petrokovets ML, Kovalev AV. Tribology of polymers: adhesion, friction, wear, and mass-transfer. *Tribol Int* 2005;38:910–21.
- [33] Rabinowicz E. Friction and wear of materials. 2nd ed. New York: Wiley; 1995.
- [34] Brostow W, Deborde J-L, Jaklewicz M, Olszynski P. Tribology with emphasis on polymers: friction, scratch resistance and wear. *J Mater Educ* 2003;25:119–32.
- [35] Brostow W, Kovacevic V, Vrsaljko D, Whitworth J. Tribology of polymers and polymer based composites. *J Mater Educ* 2010;32:273–90.
- [36] Chin I-J, Thurn-Albrecht T, Kim H-C, Russell TP, Wang J. On exfoliation of montmorillonite in epoxy. *Polymer* 2001;42(13):5947–52.
- [37] Becker O, Varley R, Simon G. Morphology, thermal relaxations and mechanical properties of layered silicate nanocomposites based upon high-functionality epoxy resins. *Polymer* 2002;43(16):4365–73.
- [38] Akbari B, Bagheri R. Deformation mechanism of epoxy/clay nanocomposite. *Eur Polym J* 2007;43:782–8.
- [39] Garcia del Cid MA, Prolongo MG, Salom C, Arribas C, Sanchez-Cabezudo M, Masegosa RM. The effect of stoichiometry on curing and properties of epoxy-clay nanocomposites. *J Thermal Anal Calorim* 2012;108:741–9.
- [40] Steijn RP. Friction and wear. In: Brostow W, Corneliussen RD, editors. Failure of plastics. Munich – New York: Hanser; 1986. p. 356–92.
- [41] Jawahar P, Gnanamoorthy R, Balasubramanian M. Tribological behaviour of clay-thermoset polyester nanocomposites. *Wear* 2006;261:835–40.
- [42] Khedkar J, Negulescu L, Meletis EI. Sliding wear behavior of PTFE composites. *Wear* 2002;252:361–9.
- [43] Houdalakis G, Gotsis AD. Permeability of polymer/clay nanocomposites: a review. *Eur Polym J* 2009;45:967–84.
- [44] Kopczyńska A, Ehrenstein GW. Polymeric surfaces and their true surface tension in solids and melts. *J Mater Educ* 2007;29:325.
- [45] Desai RC, Kapral R. Dynamics of self-organized and self-assembled structures. Cambridge – New York: Cambridge University Press; 2009.
- [46] Michler GH, Balta-Calleja FJ. Nano- and Micromechanics of polymers: structure modification and improvement of properties. Munich – Cincinnati: Hanser; 2012.